***Electronic Supplementary Information (ESI):***

# Multi-cation crosslinked anion exchange membranes from microporous Tröger's base copolymers

Chuan Hu, Qiugen Zhang*, Chenxiao Lin, Zhen Lin, Ling Li, Faizal Soyekwo, Aimei Zhu and Qinglin Liu

**Contents** **Page**

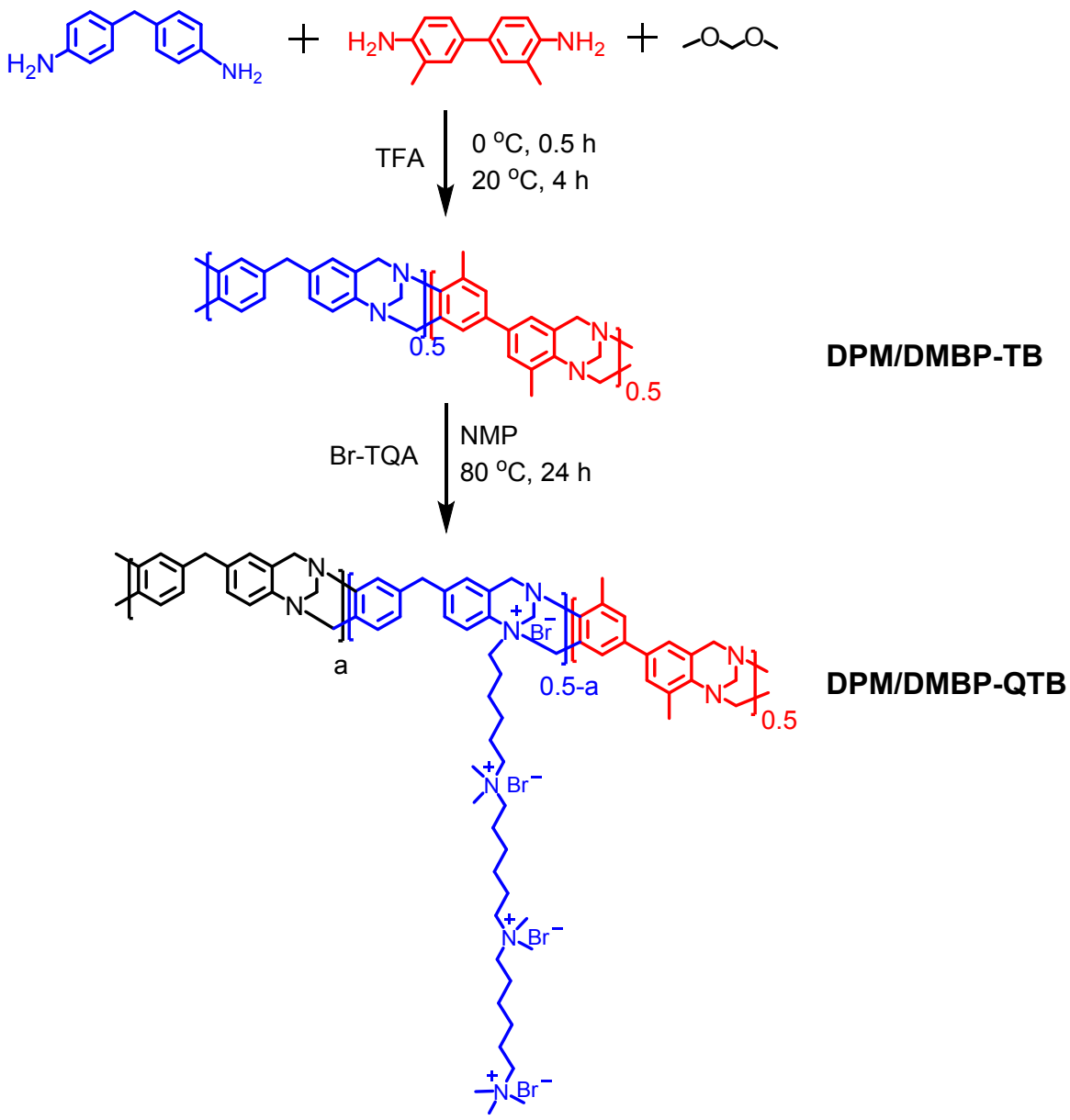


**Scheme S1** Synthetic process of the DPM/DMBP-QTB copolymer.

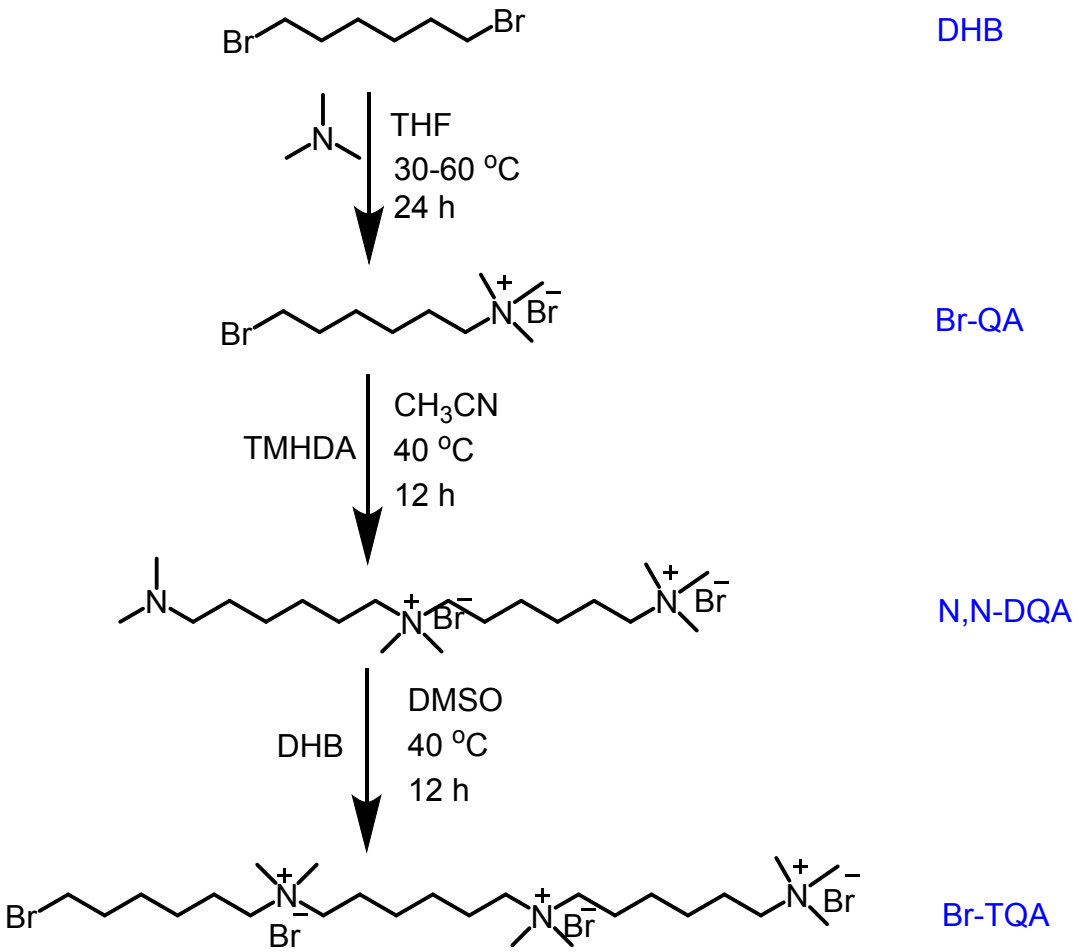


**Scheme S2** Synthesis of the Br-TQA.

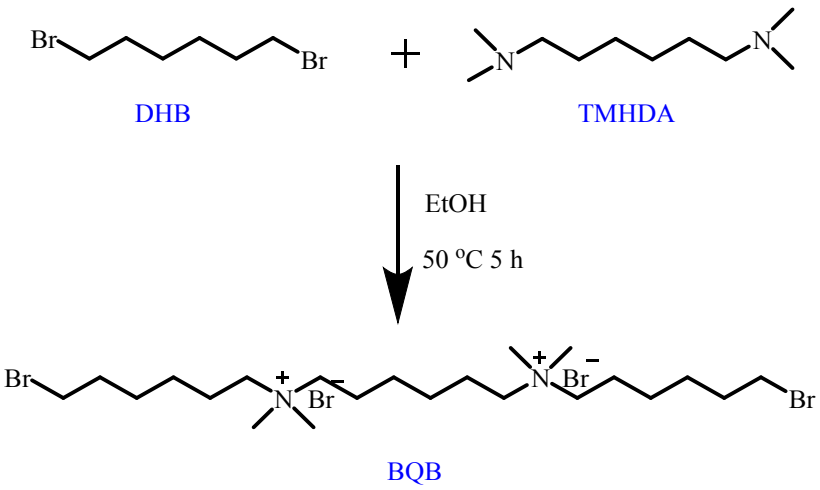


**Scheme S3** Synthesis of the BQB.

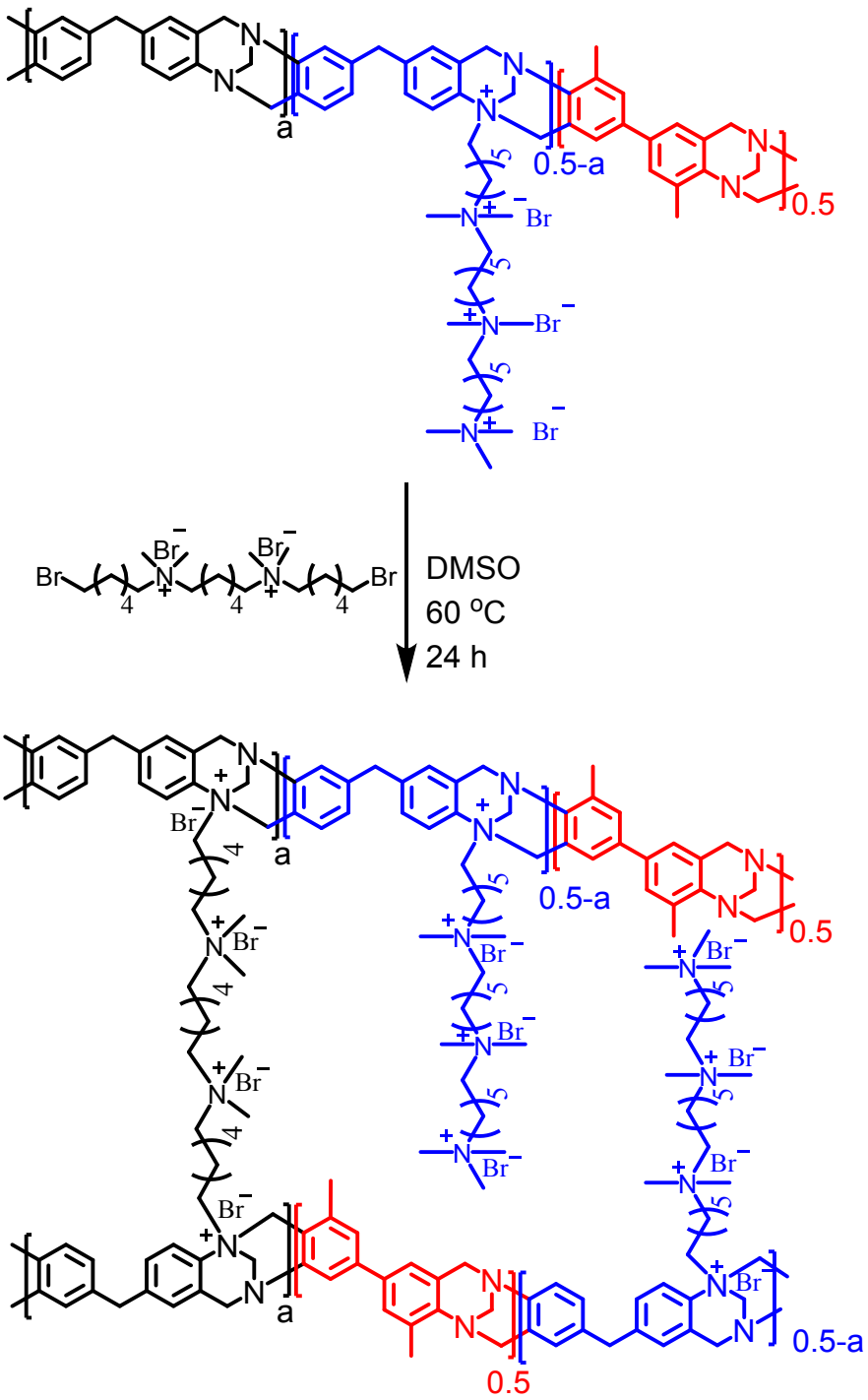


**Scheme S4** The reaction route of the crosslinked DPM/DMBP-QTB AEMS.

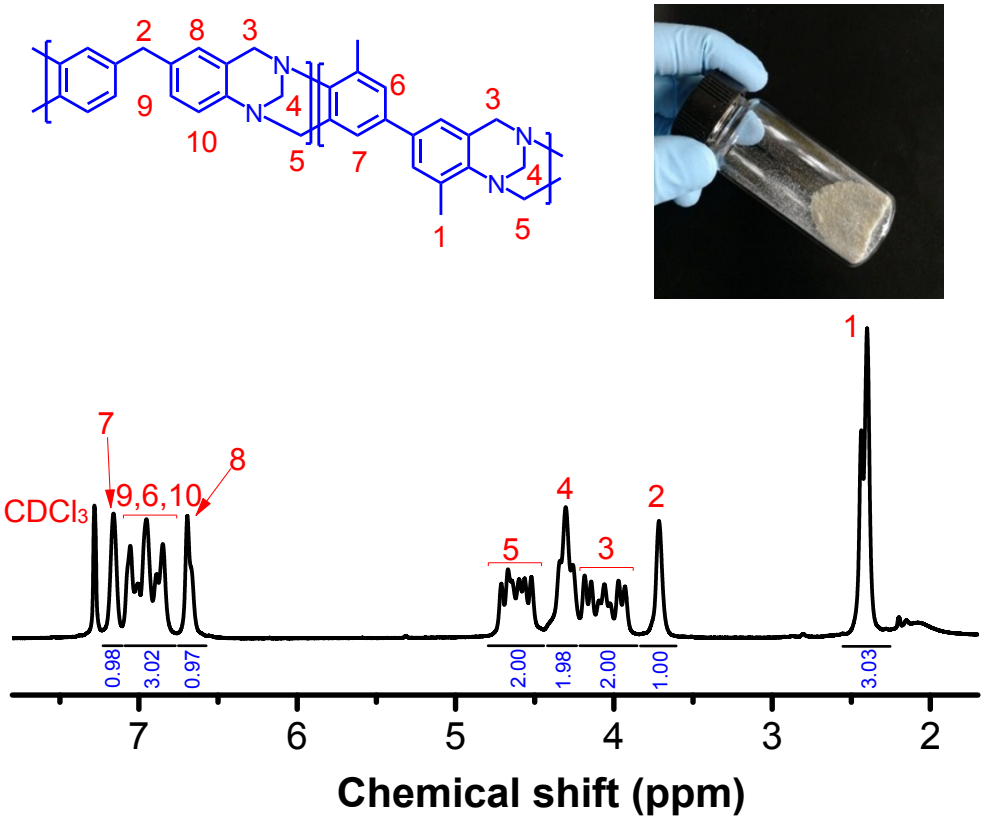


**Fig. S1** The $^{1}$H NMR spectrum and digital photo of the DPM/DMBP-TB copolymer.

$^{1}$H NMR (400 MHz, $CDCl_3$ $\delta$): 7.16 (s, 2H, Ar H), 7.05 (d, $J$ = 7.6 Hz, 2H, Ar H), 6.95 (s, 2H, Ar H), 6.85 (d, 2H, $J$ = 7.6 Hz, Ar H), 6.70 (s, 2H, Ar H), 4.62 (m, 4H, $CH_2$), 4.28 (s, 4H, $CH_2$), 4.06 (m, 4H, $CH_2$), 3.71(m, 2H, $CH_2$), 2.42(d, 6H, $CH_3$).

The peak emerging from δ = 6.70 − 7.16 is in response to the characteristic aromatic protons on the benzene ring. The signal at δ = 2.42 is associated with the protons of methyl on the benzene rings (Ar−$CH_3$) that comes from monomer 4,4'-diamine-3,3'-dimethyl-biphenyl (DMBP). The signal at δ = 3.71 is attributed to the methylene group between two benzene rings (Ar−$CH_2$−Ar) which is associated with monomer 4,4'-Diaminodiphenylmethane (DPM).

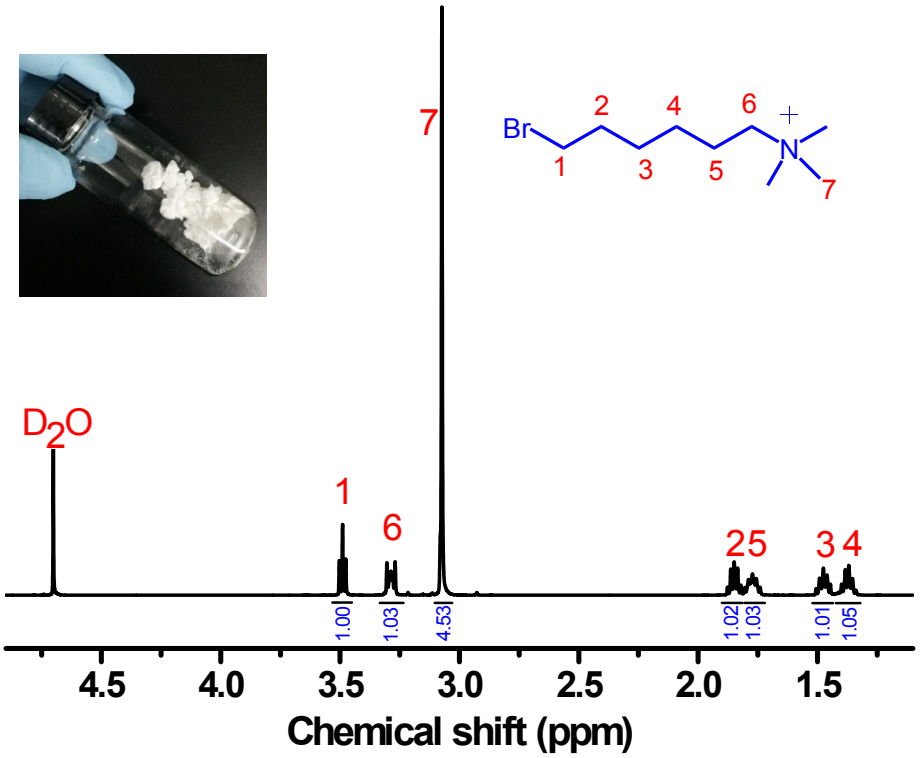


**Fig. S2** The $^{1}$H NMR spectrum and digital photo of the Br-QA.

$^{1}$H NMR (400 MHz, $D_2O$, $\delta$): 1.37 (h, $J$ = 7.2, 6.5 Hz, 2H, $CH_2$), 1.47 (m, 2H, $CH_2$), 1.60 (m, 2H, $CH_2$), 1.76 (m, 2H, $CH_2$), 1.85 (p, $J$ = 6.8 Hz, 2H, $CH_2$), 3.07 (s, 9H, $CH_3$), 3.28 (m, 2H, $CH_2$), 3.48 (t, $J$ = 6.7 Hz, 2H, $CH_2$).

The peak at δ = 3.07 (s, 9H, $CH_3$) is associated with the quaternary ammonium groups from trimethylamine. The single at δ = 1.37 − 1.85 ppm is attributed to alkyl chain from DHB.

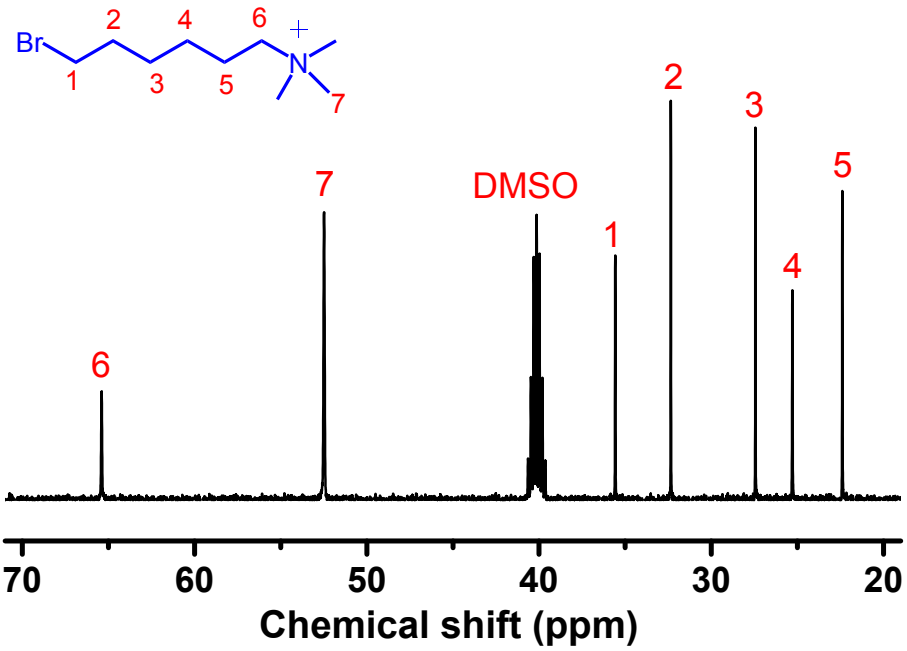


**Fig. S3** The $^{13}$C NMR spectrum of the Br-QA.

$^{13}$C NMR (400 MHz, DMSO-*d6*): $\delta$ (ppm) 65.40, 52.48, 35.57, 32.35, 27.44, 25.29, 22.39.

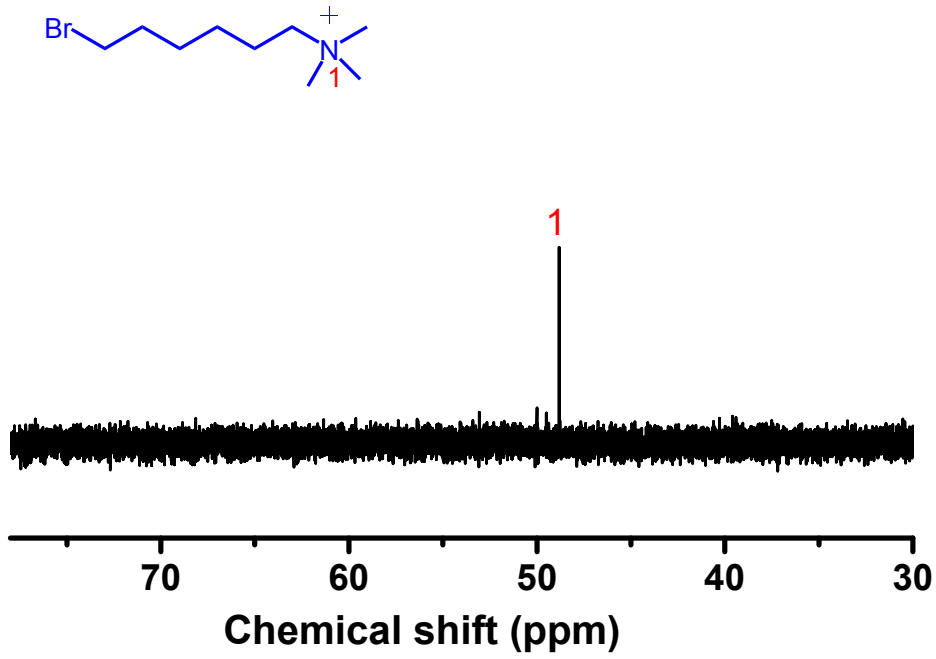


**Fig. S4** The $^{15}N$ NMR spectrum of Br-QA.

$^{15}N$ NMR (600 MHz, $D_2O$): $\delta$ (ppm) 48.77

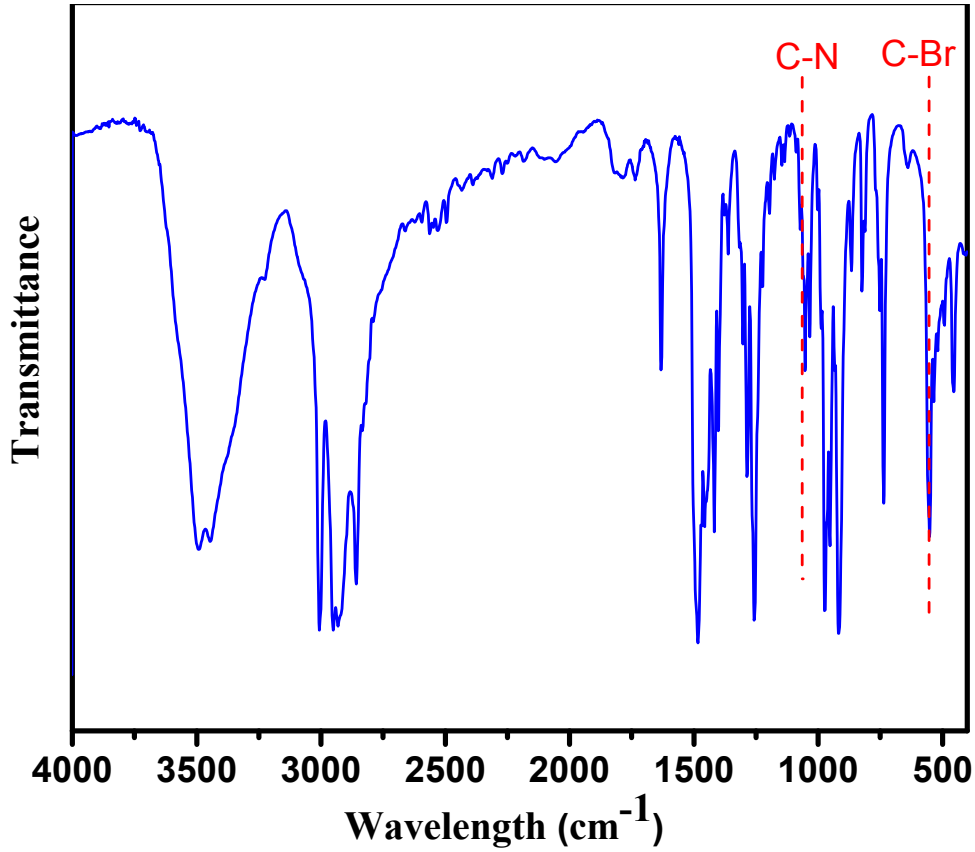


**Fig. S5** FT-IR spectrum of the Br-QA at 25 °C (KBr).

FT-IR (KBr): $\nu$ ($cm^{-1}$) 3494, 3446, 3006, 2952, 2859, 1632, 1484, 1457, 1417, 1401, 1362, 1301, 1285, 1255, 1223, 1077, 1052, 1033, 972, 951, 916, 866, 823, 812, 751, 737, 639, 551, 533, 517, 492, 453.

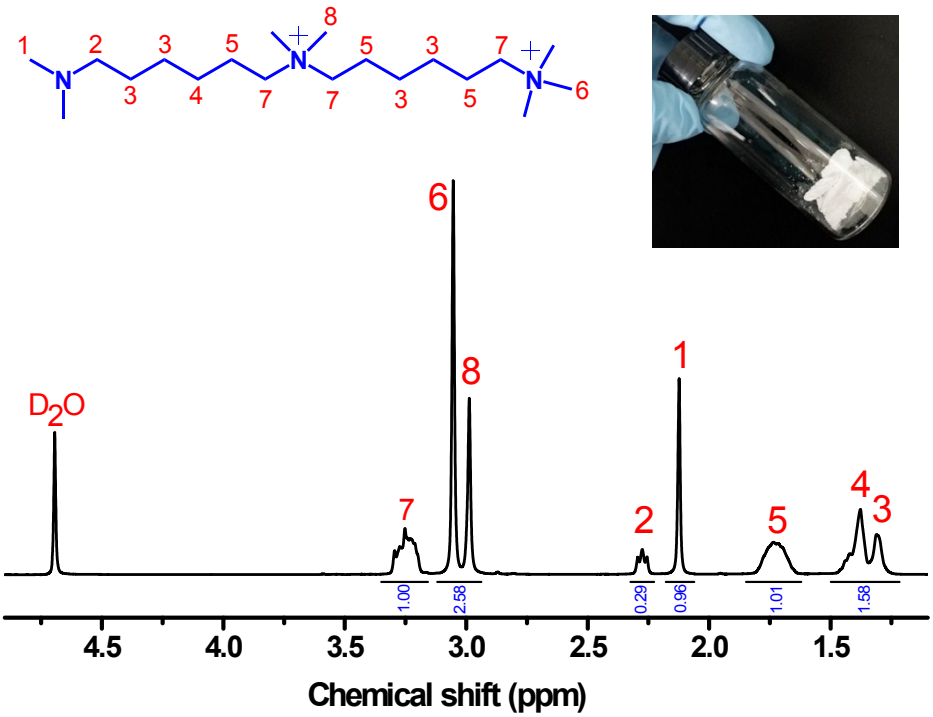


**Fig. S6** The $^1$H NMR spectrum in $D_2O$ and digital photo of the N, N-DQA.

$^1$H NMR (400 MHz, $D_2O$ $\delta$): 1.30 (m, 2H, $CH_2$), 1.40 (m, 8H, $CH_2$), 1.72 (m, 6H, $CH_2$), 2.12 (s, 6H, $CH_3$), 2.27 (m, 2H, $CH_2$), 2.98 (s, 6H, $CH_3$), 3.05 (s, 9H, $CH_3$), 3.25 (m, 6H, $CH_2$).

Compared with the spectrum of the Br-QA, the peak at $\delta$ = 3.48 (t, $J$ = 6.7 Hz, 2H, $CH_2$) disappeared. Subsequently, there were two new peaks emerged at $\delta$ = 2.12 (s, 6H, $CH_3$) and $\delta$ = 2.27 (m, 2H, $CH_2$).

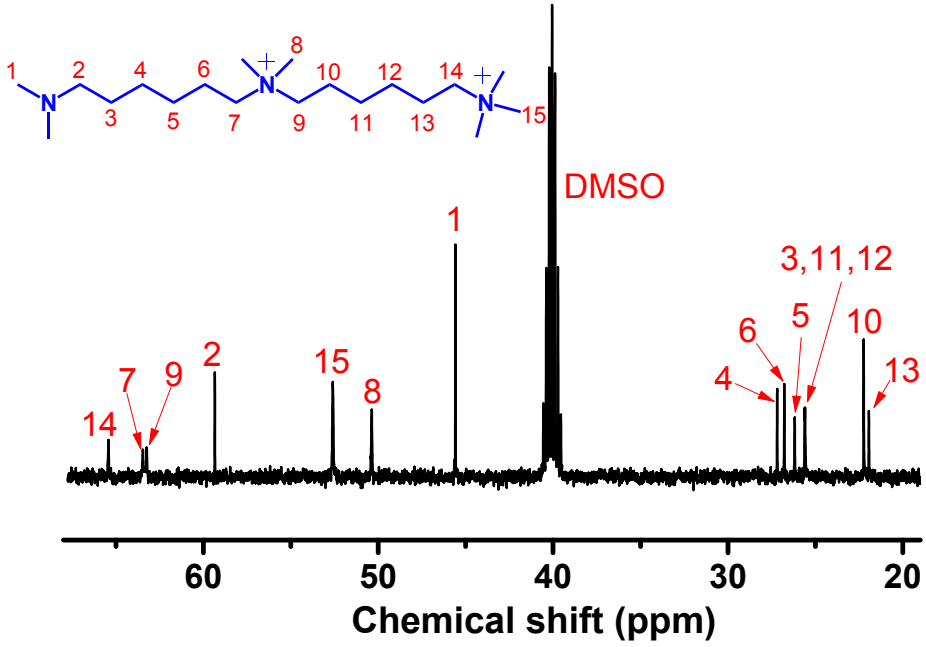


**Fig. S7** The $^{13}C$ NMR spectrum of the N, N-DQA.

$^{13}C$ NMR (400 MHz, DMSO-*d6*): $\delta$ (ppm) 65.42, 63.46, 63.23, 59.34, 52.61, 50.37, 45.58, 27.19, 26.78, 26.18, 25.59, 22.24, 21.94.

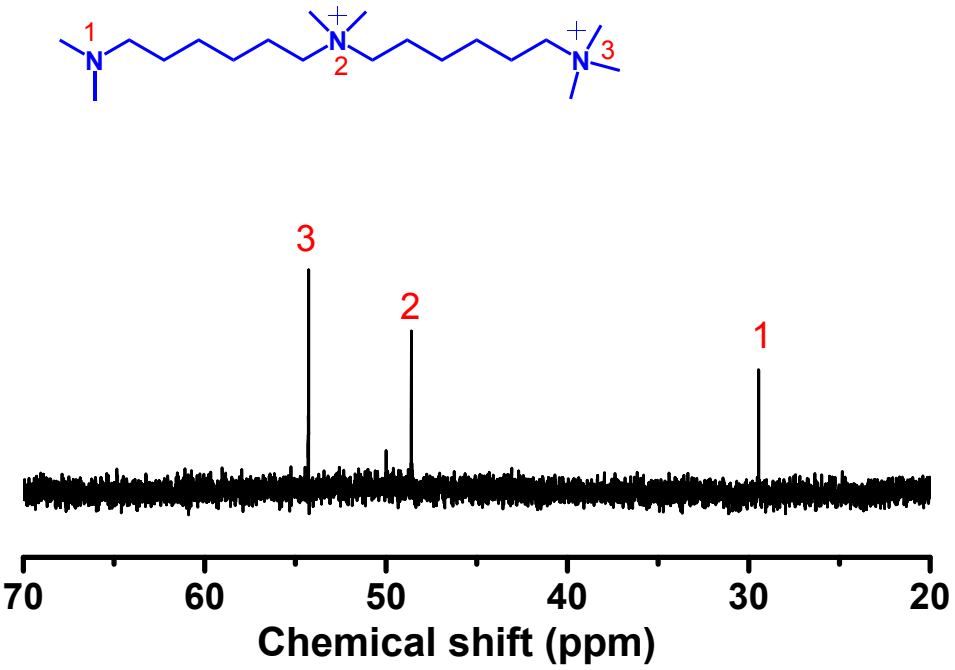


**Fig. S8** The $^{15}N$ NMR spectrum of the N, N-DQA.

$^{15}N$ NMR (600 MHz, $D_2O$): $\delta$ (ppm) 52.27, 48.61, 29.45

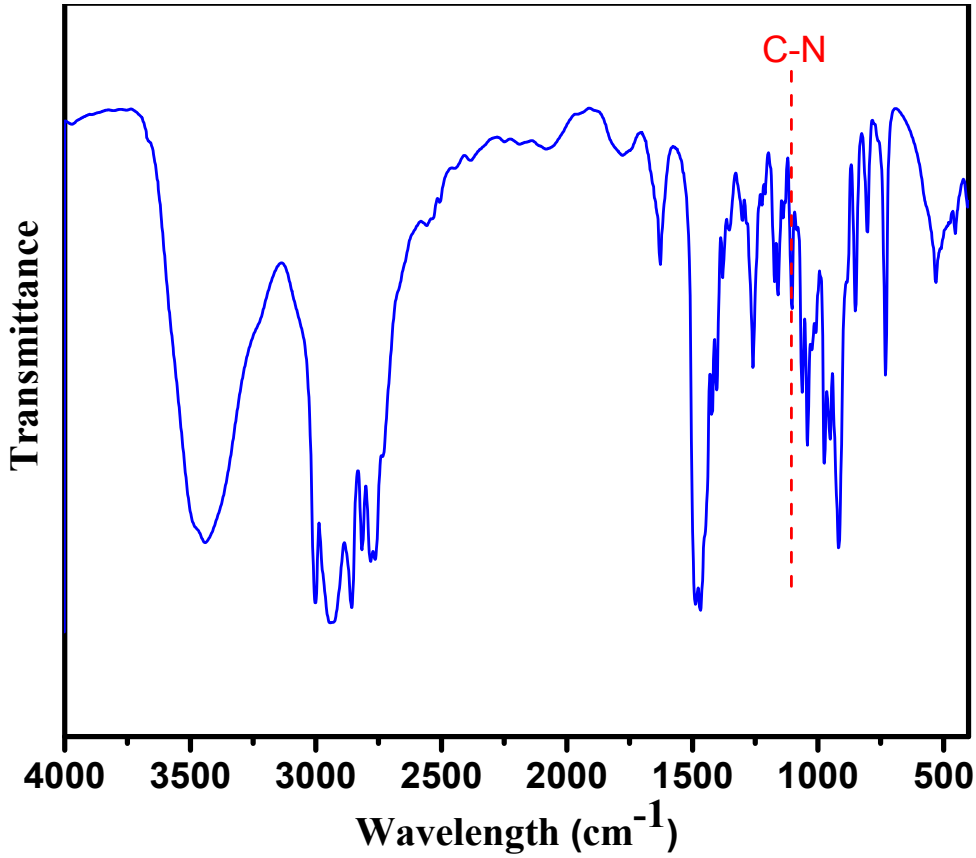


**Fig. S9** FT-IR spectrum of the N, N-DQA at 25 °C (KBr).

FT-IR (KBr): $\nu$ ($cm^{-1}$) 3440, 3001, 2936, 2852, 2817, 2781, 2764, 1782, 1629, 1485, 1467, 1422, 1402, 1379, 1354, 1300, 1258, 1223, 1209, 1172, 1158, 1103, 1062, 1042, 974, 951, 918, 850, 803, 730, 530, 453.

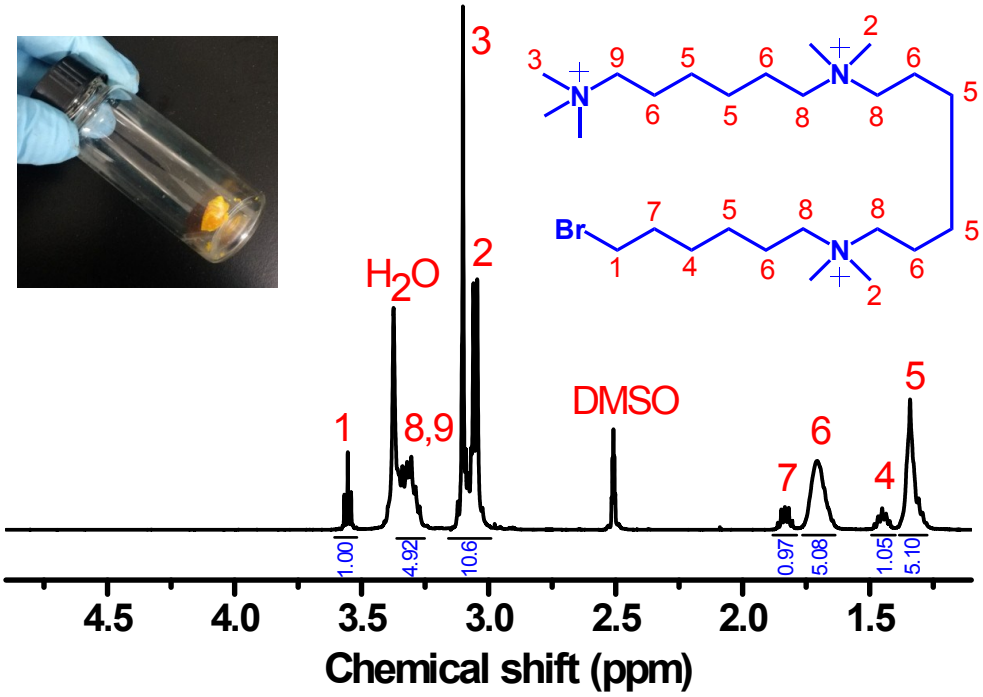


**Fig. S10** The $^{1}$H NMR spectrum and digital photo of the Br-TQA.

$^{1}$H NMR (400 MHz, DMSO-*d6* *δ*): 1.30 (m, 10H, $CH_2$), 1.45 (m, 2H, $CH_2$), 1.72 (m, 10H, $CH_2$), 1.80 (m, 2H, $CH_2$), 3.04 (s, 6H, $CH_3$), 3.06 (s, 6H, $CH_3$), 3.10 (s, 9H, $CH_3$), 3.3 (m, 10H, $CH_2$), 3.57 (t, $J$ = 6.7 Hz, 2H, $CH_2$).

Compared with the spectrum of the N, N-DQA, the single at δ = 2.27 (t, 2H, $CH_2$) disappeared. Subsequently, the peak at δ = 3.57 (t, $J$ = 6.7 Hz, 2H, $CH_2$) appeared again. Furthermore, the three peaks located at δ = 3.04 − 3.10 (s, 21H, $CH_3$) corresponded to three quaternary ammonium groups which indicated that the target product was successfully synthesized.

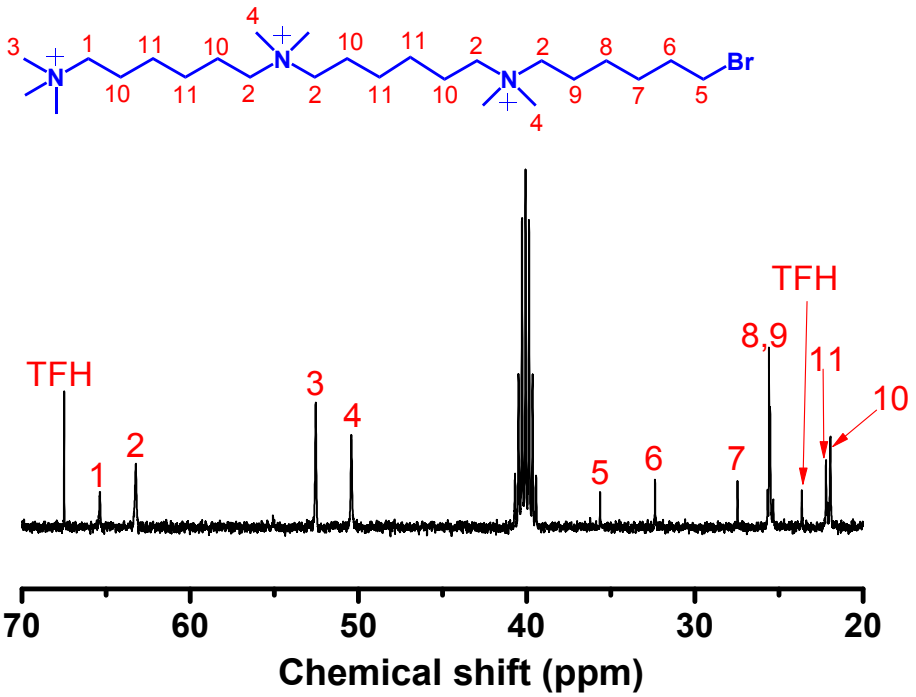


**Fig. S11** The $^{13}$C NMR spectrum of the Br-TQA.

$^{13}$C NMR (400 MHz, DMSO-*d6*): $\delta$ (ppm) 65.36, 63.23, 52.54, 50.42, 35.63, 32.37, 27.47, 25.59, 25.53, 22.21, 21.94.

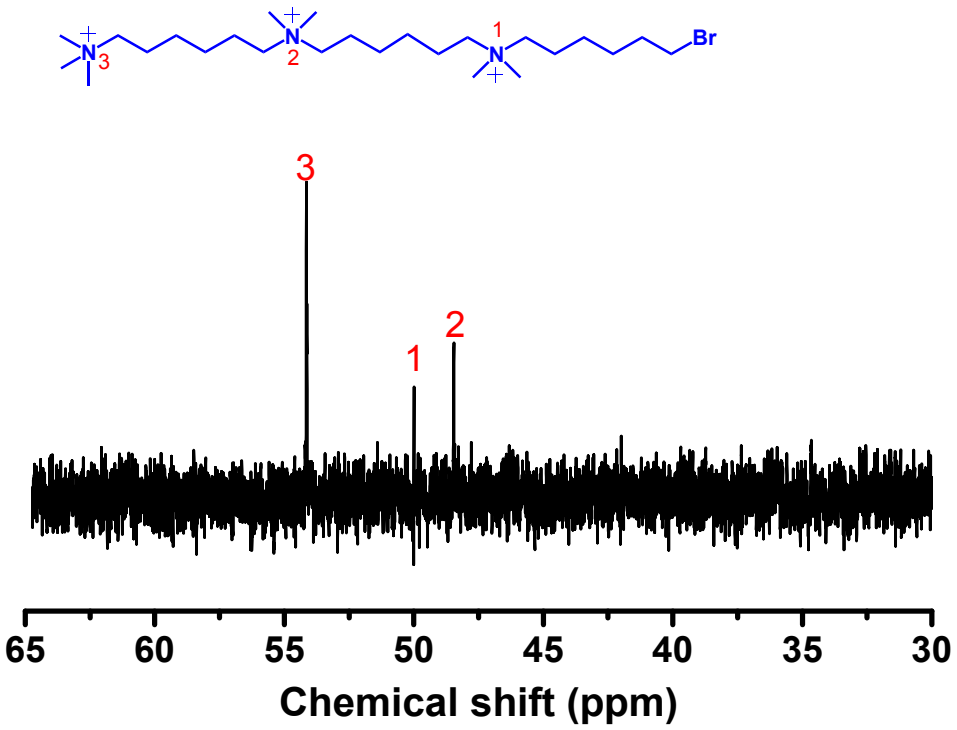


**Fig. S12** The $^{15}N$ NMR spectrum of the Br-TQA.

$^{15}N$ NMR (600 MHz, $D_2O$): $\delta$ (ppm) 54.17, 50.01, 48.44

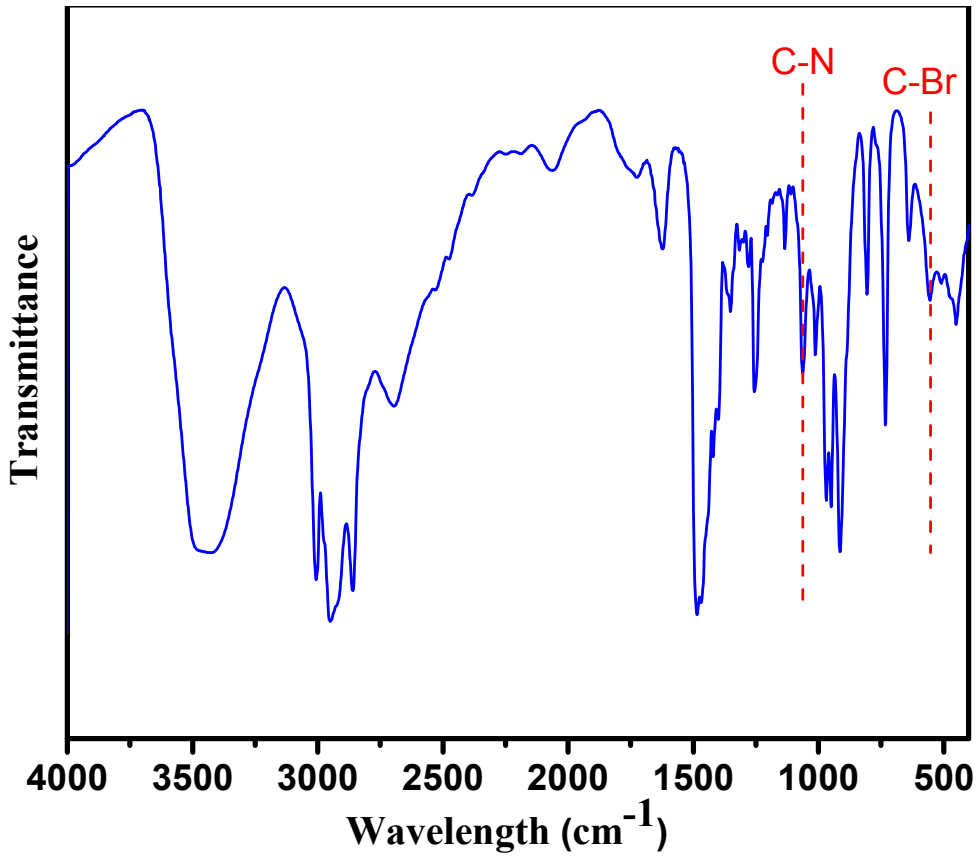


**Fig. S13** FT-IR spectrum of Br-TQA at 25 °C (KBr).

FT-IR (KBr): $\nu$ ($cm^{-1}$) 3454, 3009, 2947, 2857, 2694, 2067, 1726, 1620, 1487, 1467, 1419, 1402, 1353, 1315, 1277, 1254, 1133, 1062, 1010, 967, 950, 914, 803, 731, 637, 554, 510, 453.

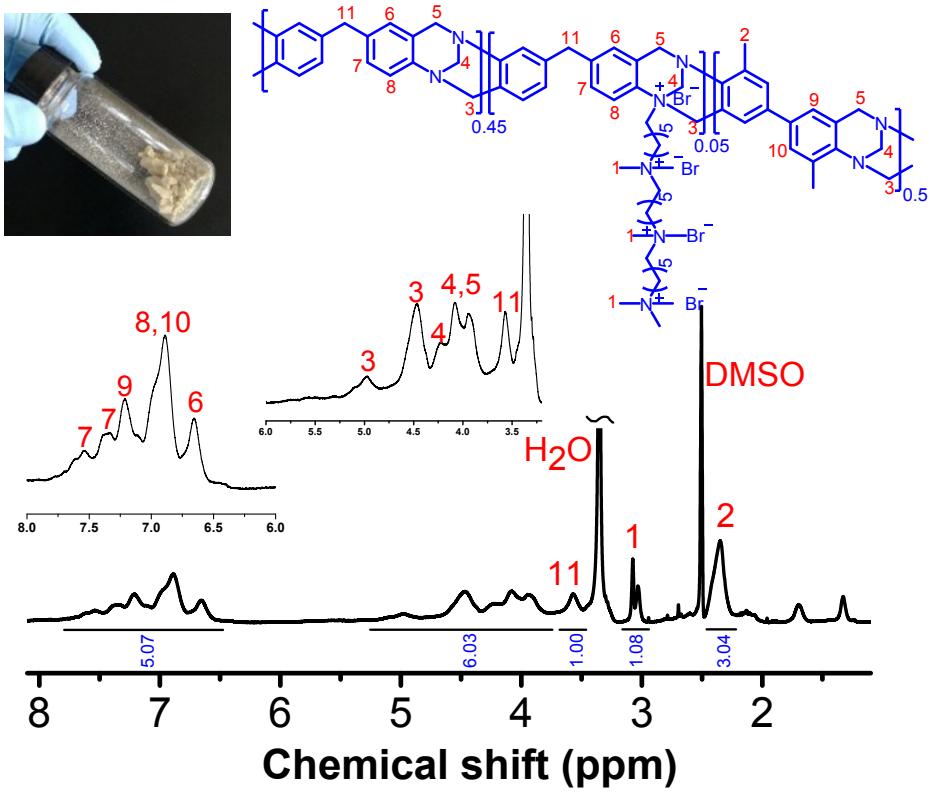


**Fig. S14** The $^{1}H$ NMR spectrum and digital photo of the DPM/DMBP-QTB copolymer.

Apparently, compared with the spectrum of the DPM/DMBP-QTB, the signal at δ = 3.04 − 3.10 (m, 21H, $CH_3$) are attributed to the quaternary ammonium groups from Br-TQA. The peaks located at δ = 1.33 − 1.70 (m, 24H, $CH_2$) were associated with the alkyl chain.

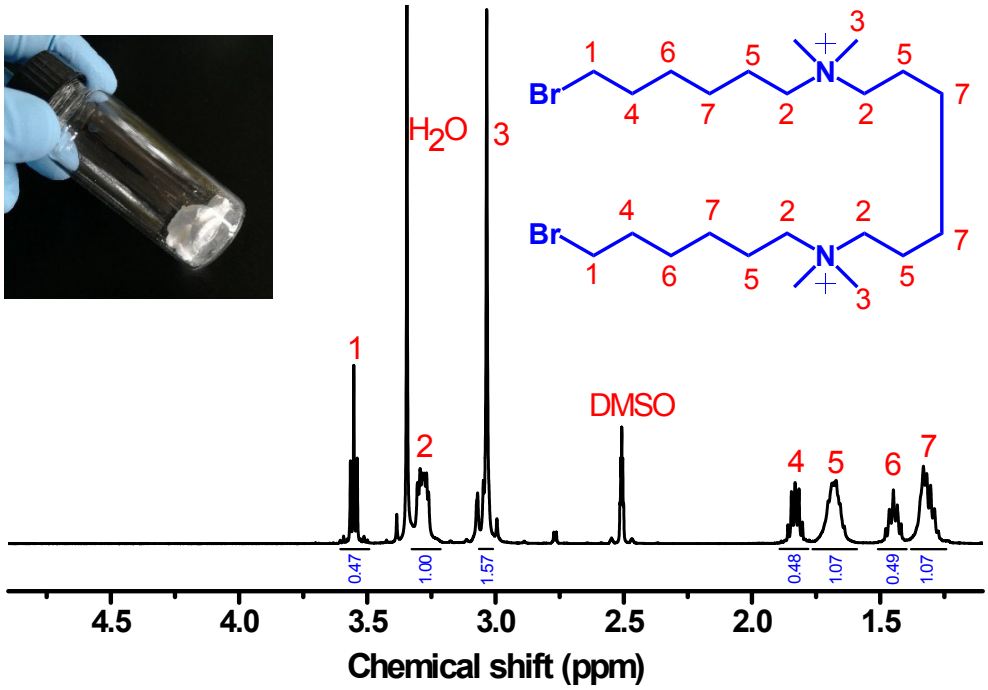


**Fig. S15** The $^{1}$H NMR spectrum and digital photo of the BQB.

$^{1}$H NMR (400 MHz, DMSO-d6, $\delta$): 1.30 (m, 8H, $CH_2$), 1.45 (dq, $J$ = 9.0, 7.2 Hz 4H, $CH_2$), 1.69 (m, 8H, $CH_2$), 1.83 (dt, $J$ = 14.8, 6.8 Hz 4H, $CH_2$), 3.03 (s, 12H, $CH_3$), 3.28 (dt, $J$ = 12.8, 4.6 Hz, 8H, $CH_2$), 3.55 (t, $J$ = 6.7 Hz, 4H, $CH_2$)

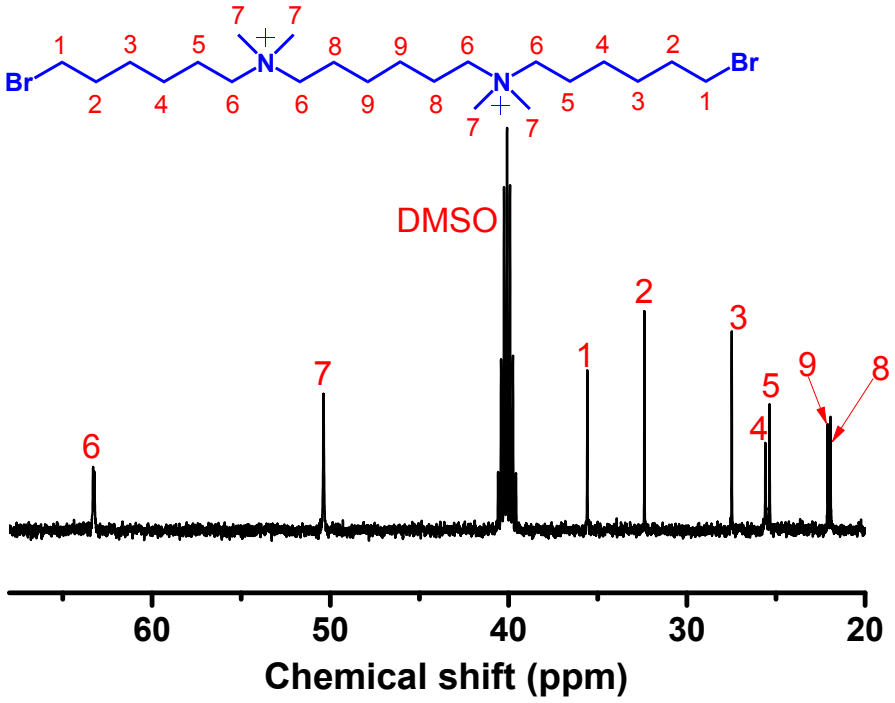


**Fig. S16** The $^{13}$C NMR spectrum of the BQB.

$^{13}$C NMR (400 MHz, DMSO-*d6*): $\delta$ (ppm) 63.29, 50.37, 35.58, 32.38, 27.48, 25.59, 25.35, 22.10, 21.94.

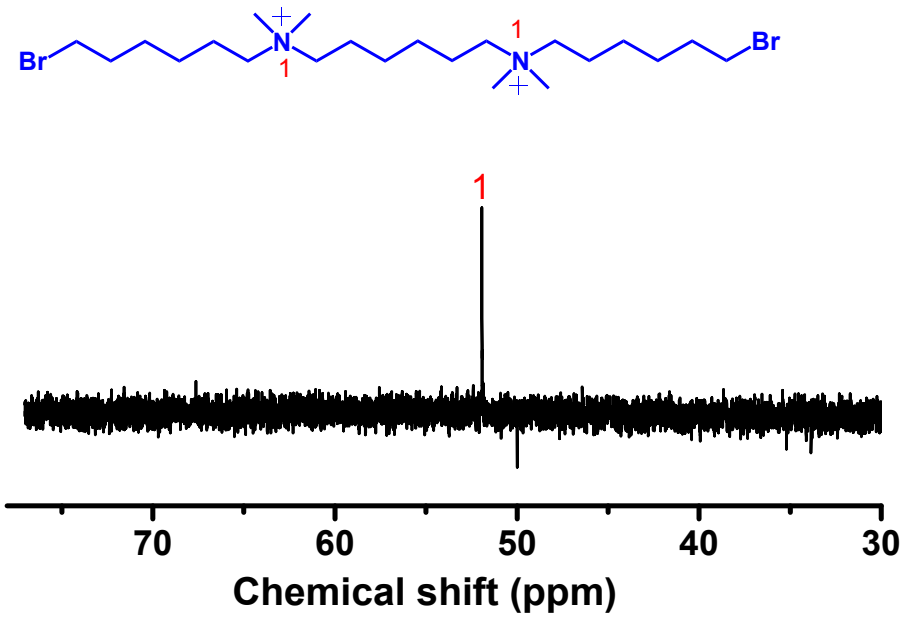


**Fig. S17** The $^{15}N$ NMR spectrum of the BQB.

$^{15}N$ NMR (600 MHz, $D_2O$): $\delta$ (ppm) 51.92.

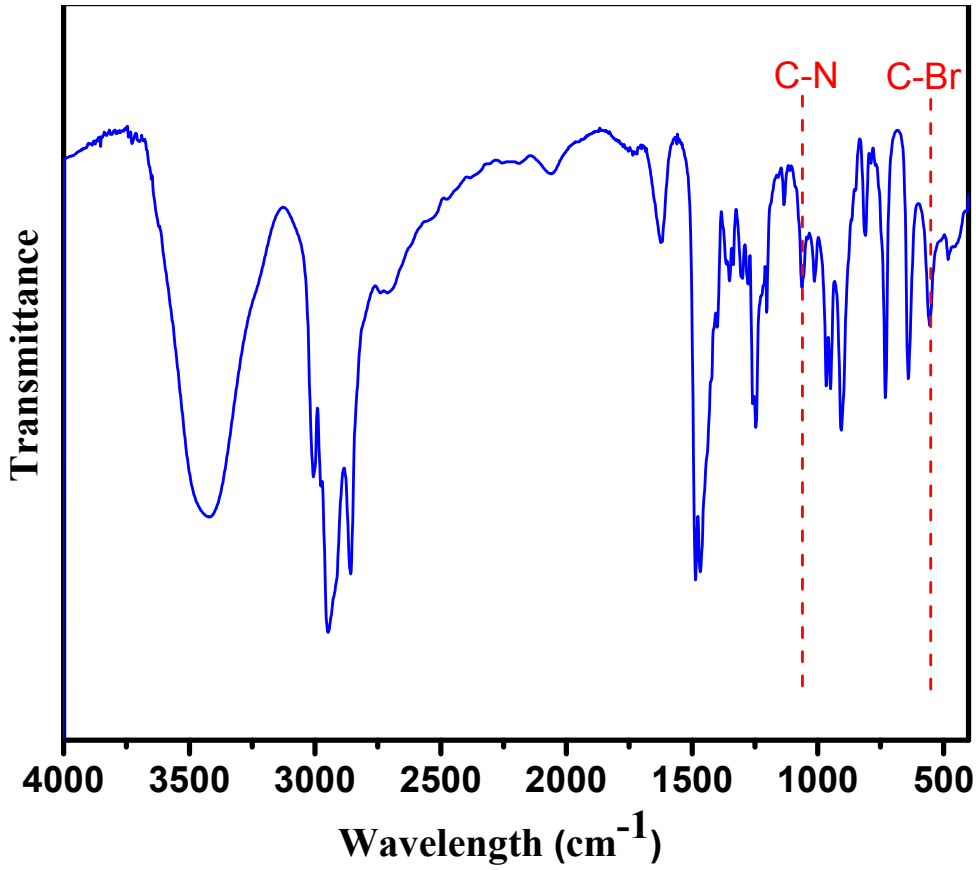


**Fig. S18** FT-IR spectrum of the BQB at 25 °C (KBr).

FT-IR (KBr): $\nu$ ($cm^{-1}$) 3454, 3009, 2947, 2857, 2694, 2067, 1726, 1620, 1487, 1467, 1419, 1402, 1353, 1315, 1277, 1254, 1133, 1062, 1010, 967, 950, 914, 803, 731, 637, 554, 510, 453.

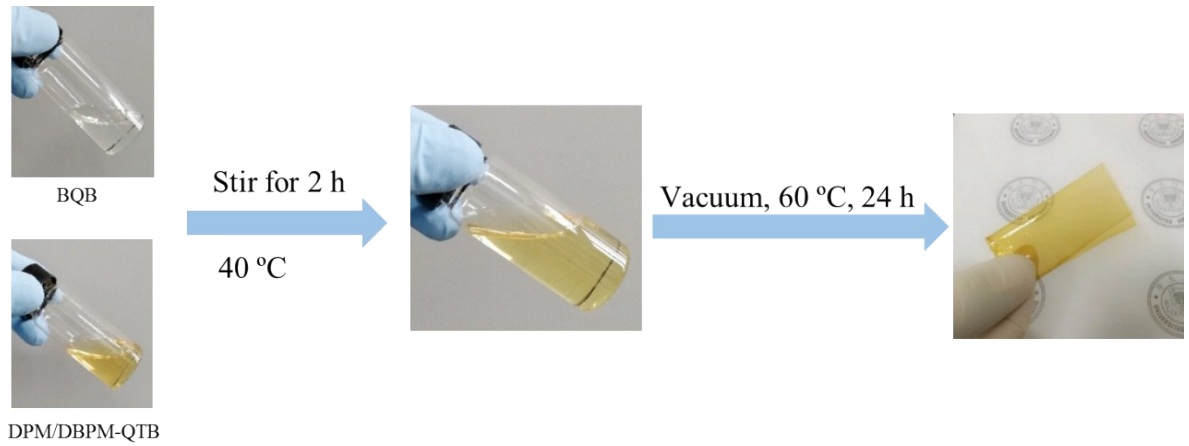


**Fig. S19** The preparation process of the crosslinked DPM/DMBP-QTB AEMs.

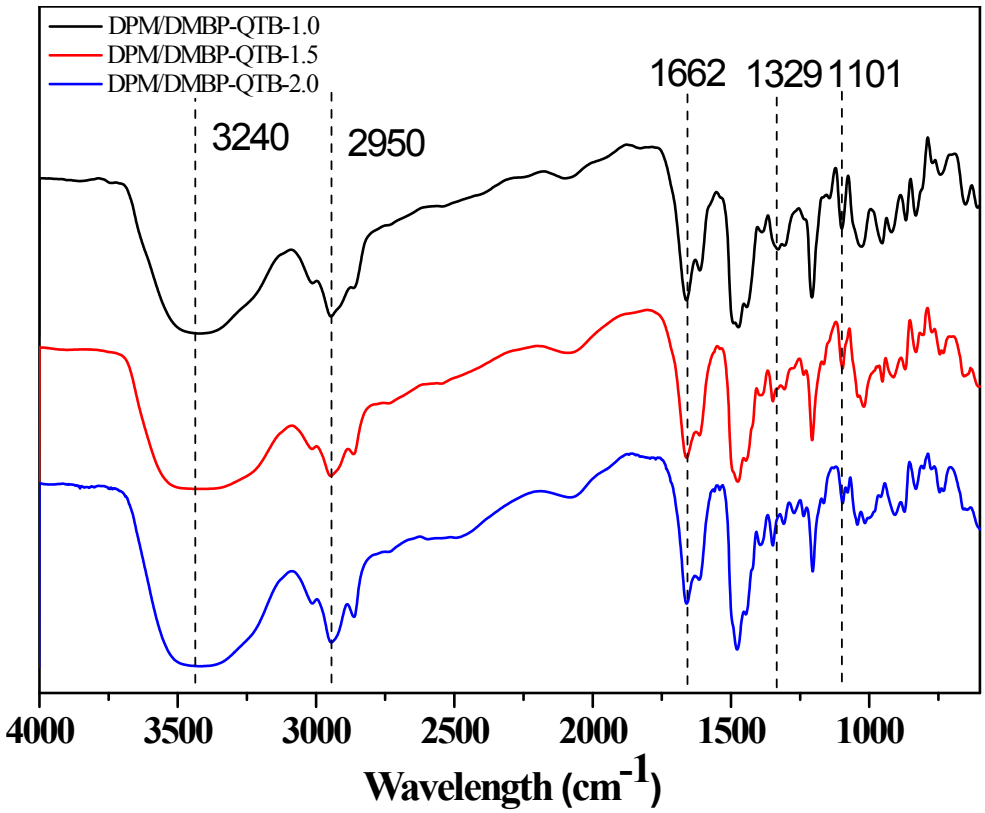


**Fig. S20** FT-IR spectra of the crosslinked DPM/DMBP-QTB AEMs.

The broad vibration bands at 3420 $cm^{-1}$ is contributed to –OH groups that comes from the bound water.[1] The strong single peak near 2950 $cm^{-1}$ is associated with the Stretching vibration of $–CH_2–$ group.[2] The peaks at 1662 $cm^{-1}$ is the bending vibration of benzene ring. In addition, the peaks at 1329 $cm^{-1}$ and 1101 $cm^{-1}$ are assigned to the C–N and $C–N^+$ groups, respectively.[3–5]

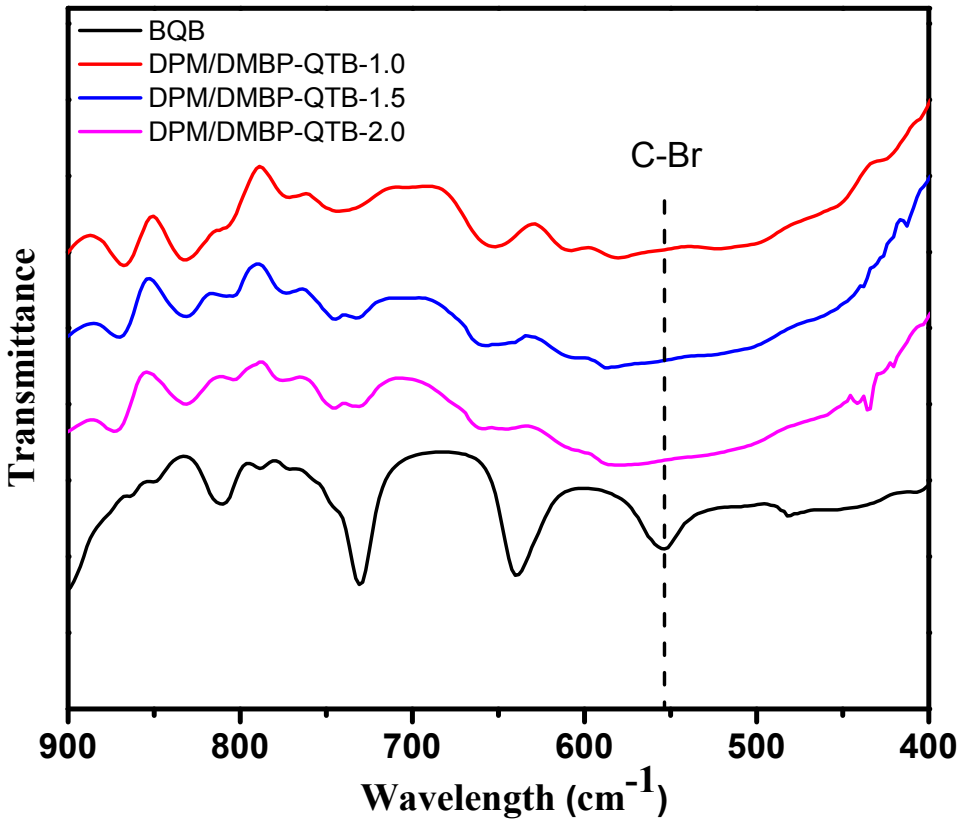


**Fig. S21** FT-IR spectra of the crosslinked DPM/DMBP-QTB AEMs and BQB.

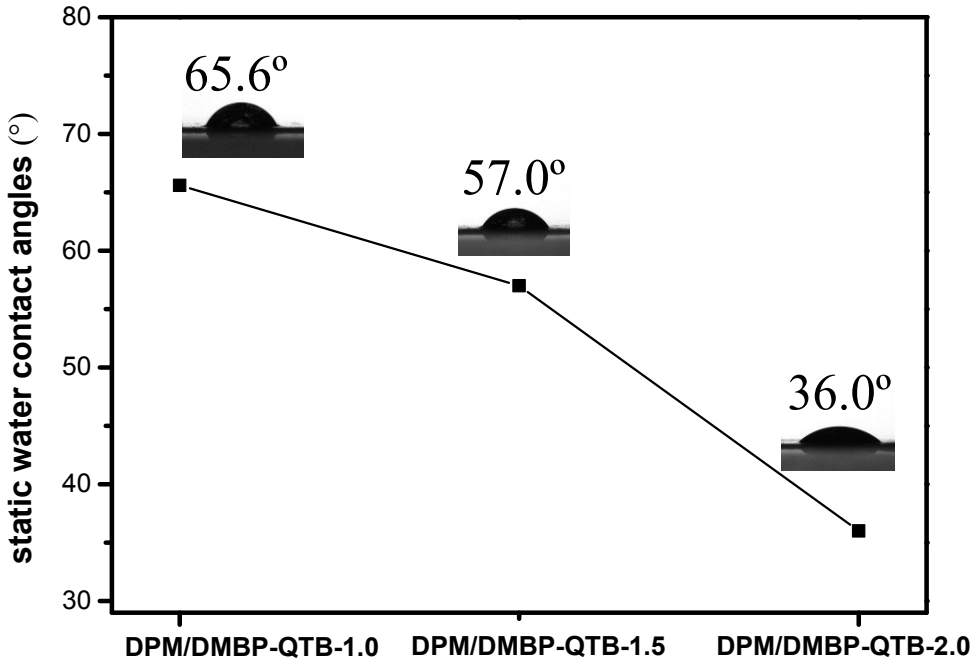


**Fig. S22** The water contact angles of the crosslinked DPM/DMBP-QTB AEMs at 25 ˚C.

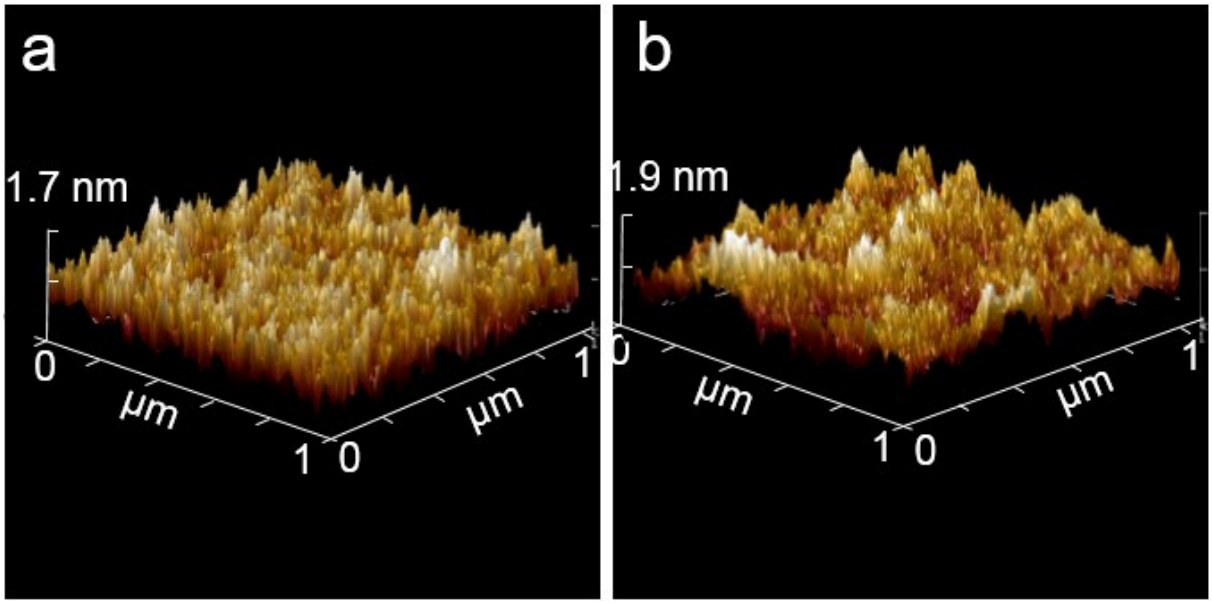


**Fig. S23** 3D AFM surface topographic of the DPM/DMBP-QTB-1.0 (a) / 2.0 (b) membranes.

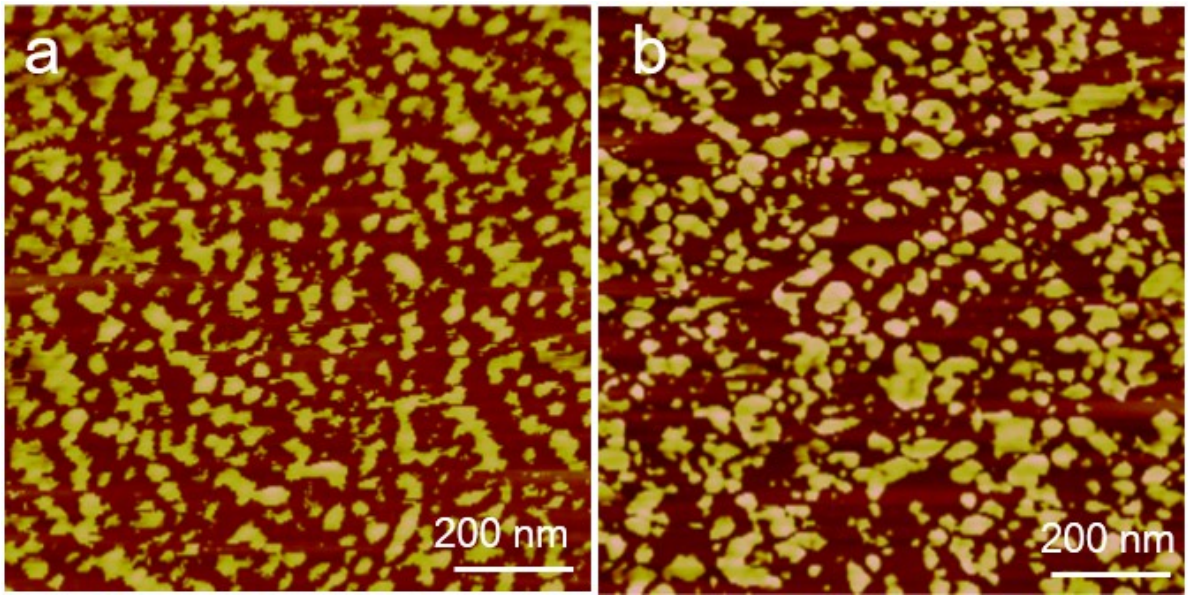


**Fig. S24** AFM phase images of the membrane DPM/DMBP-QTB-1.0 (a) /2.0 (b).

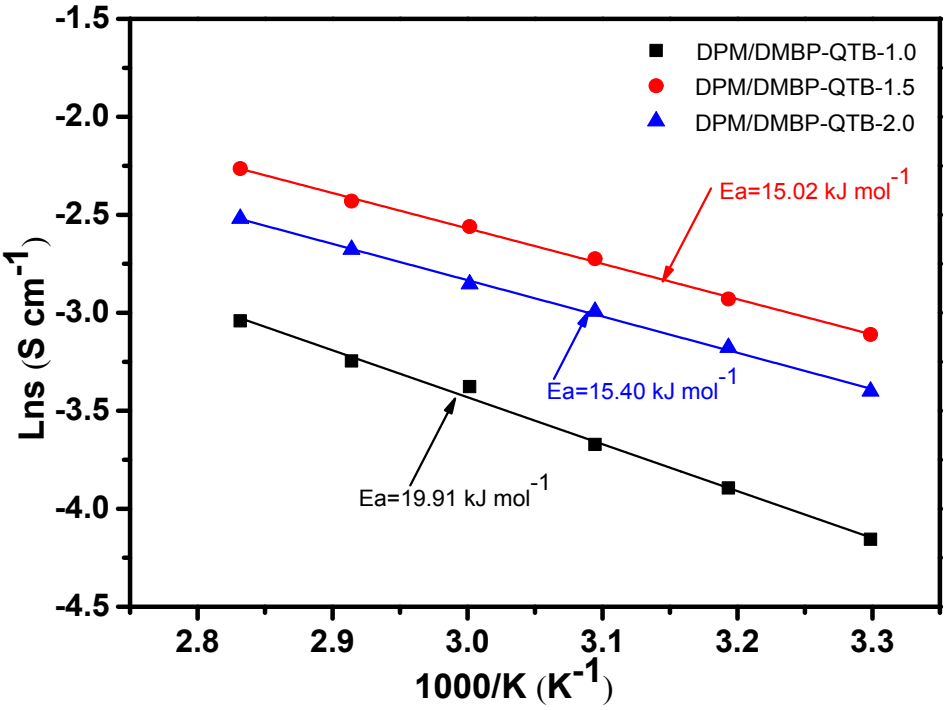


**Fig. S25** The activation energy (*Ea*) of the crosslinked DPM/DMBP-QTB AEMs.

The relationship between the conductivity and temperature can be measured by *Ea*. The *Ea* for ionic transport can be caculated by Arrhenius equation ($Ln\sigma = Ln\sigma_0 - \frac{E_a}{RT}$), where σ is the conductivity of membrane, $\sigma_0$ is the frequency factor which is independent of temperature, R

is the universal gas constant (8.314 J $mol^{-1}$ $K^{-1}$) and T is the absolute temperature.[6]

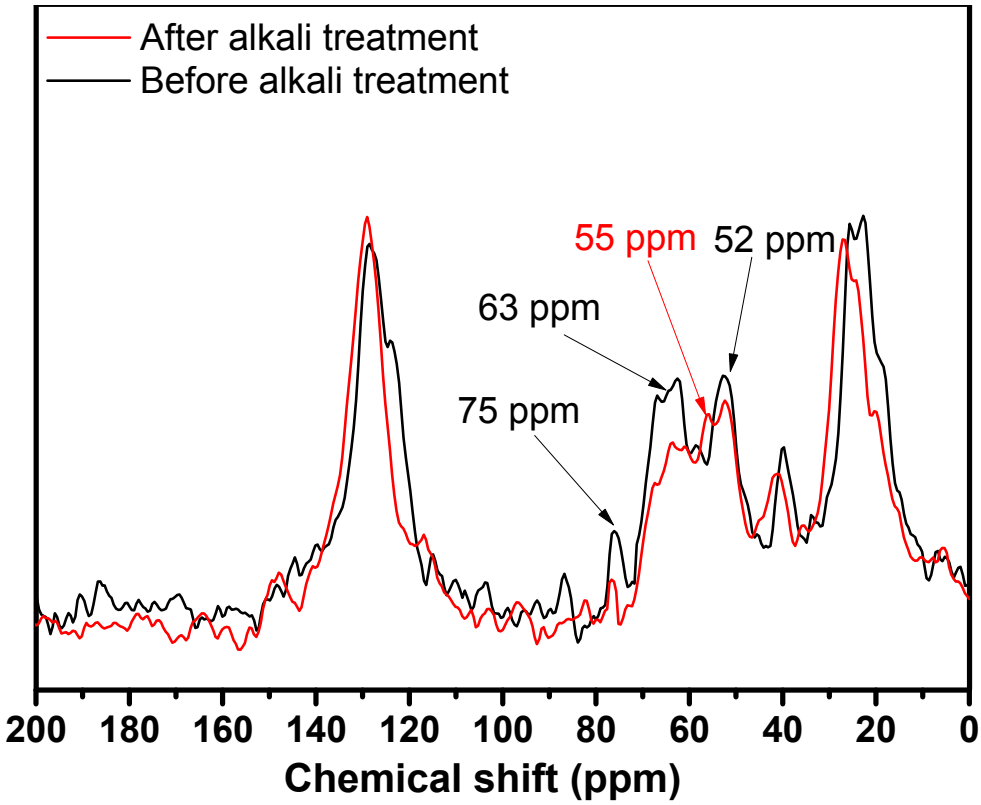


**Fig. S26** The solid state $^{13}C$ NMR spectra for the DPM/DMBP-QTB-1.5 membrane before and after alkaline ability test.

The $^{13}C$ Cross polarization/magic angle spinning ($^{13}C$ CP/MAS) solid state spectra were recorded on a Bruker Advance III 400 spectrometer. The signals around 128 ppm correspond to carbon of benzene. The peak at 75 ppm is ascribed to $-N^{+}-CH_2-N-$ in the backbone. The peaks around 63 ppm are associated with the $-N^{+}-CH_2-$ groups in the side chain. The peak located at 55 ppm is contribute to the $-N-CH_2-Ar$ groups. The peak at 52 ppm is ascribed to $-(CH_3)_2N^{+}-$ groups.

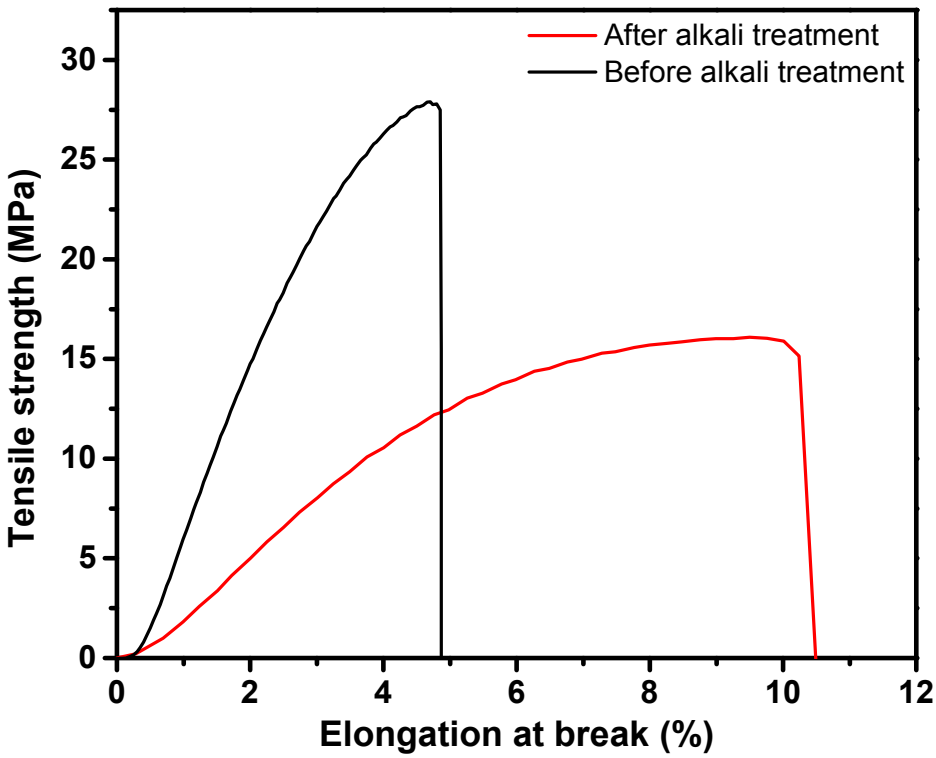


**Fig. S27** The mechanical properties of the DPM/DMBP-QTB-1.5 membrane before and after alkali resistance test.

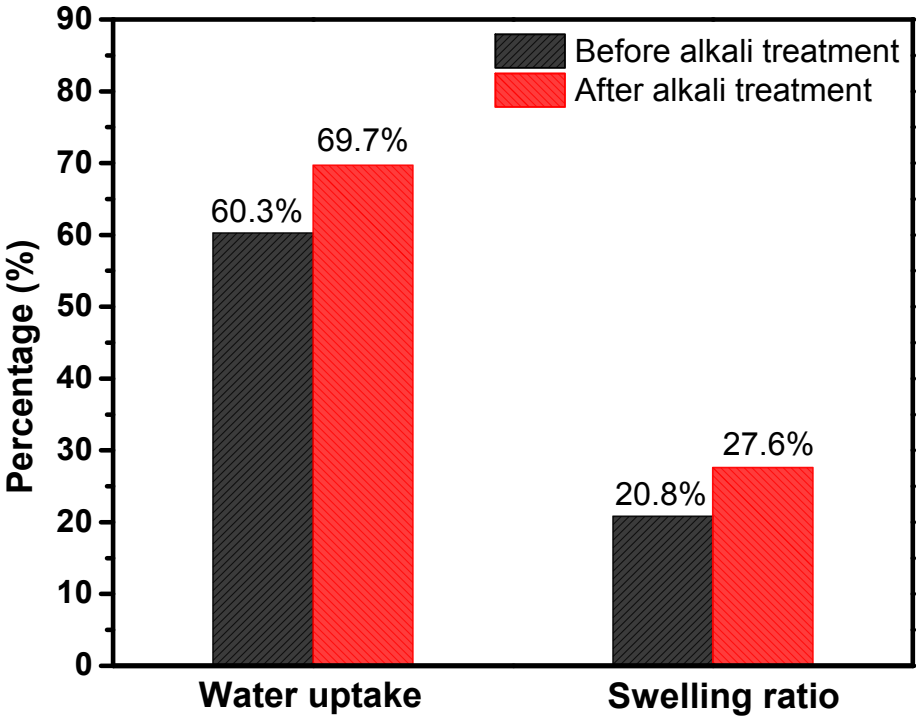


**Fig. S28** The water uptake and swelling ratio of the DPM/DMBP-QTB-1.5 membrane before and after alkali resistance test.

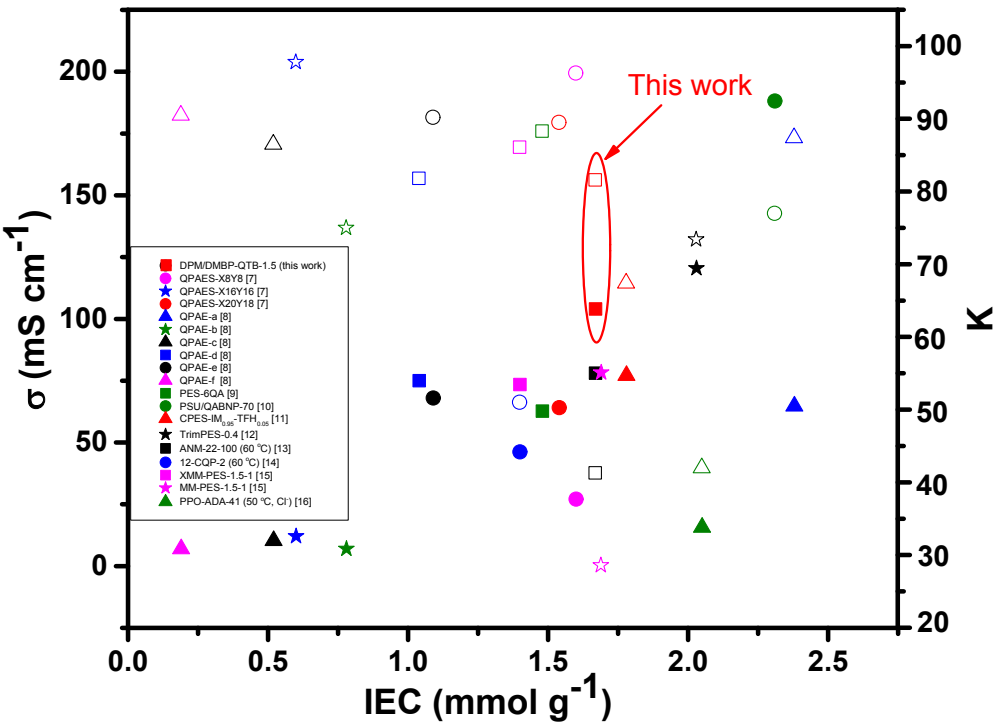


**Fig. S29** The conductivity, stability factor and IEC of DPM/DMBP-QTB-1.5 and other cross-linked AEMs reported recently.[7-16] The hollow symbols and solid symbols represent the stability factor and conductivity, respectively.

## References


[1] W.-H. Pan, S. J. Lue, C.-M. Chang, Y.-L. Liu, *J. Membr. Sci.* **2011**, 376, 225.

[2] C. G. Arges, L. Wang, M. s. Jung, V. Ramani, *J. Electrochem. Soc.* **2015**, 162, F686.

[3] Y. Cui, Y. Liu, J. Liu, J. Du, Y. Yu, S. Wang, Z. Liang, J. Yu, *Polym. Chem.* **2017**, 8, 4842.

[4] J. Han, L. Zhu, J. Pan, T. J. Zimudzi, Y. Wang, Y. Peng, M. A. Hickner, L. Zhuang, *Macromolecules* **2017**, 50, 3323

[5] F. Ishiwari, N. Takeuchi, T. Sato, H. Yamazaki, R. Osuga, J. N. Kondo, T. Fukushima, *ACS Macro Letters* **2017**, 6, 775.

[6] D. Guo, Y. Z. Zhuo, A. N. Lai, Q. G. Zhang, A. M. Zhu, Q. L. Liu, *J.Membr. Sci.* **2016**, 518, 295

[7] X. Li, Q. Liu, Y. Yu and Y. Meng, *J. Membr. Sci.,* 2014, **467**, 1-12.

[8] X. Li, Y. Yu, Q. Liu and Y. Meng, *ACS Appl. Mater. Inter.*, 2012, 4, 3627-3635.

[9] C. X. Lin, X. L. Huang, D. Guo, Q. G. Zhang, A. M. Zhu, M. L. Ye and Q. L. Liu, *J. Mater. Chem. A*, 2016, **4**, 13938-13948.

[10] G. He, M. Xu, Z. Li, S. Wang, S. Jiang, X. He, J. Zhao, Z. Li, X. Wu, T. Huang, C. Chang, X. Yang, H. Wu and Z. Jiang, *ACS Appl. Mater. Inter.*, 2017, 9, 28346-28354.

[11] C. X. Lin, Y. Z. Zhuo, E. N. Hu, Q. G. Zhang, A. M. Zhu and Q. L. Liu, *J. Membr. Sci.*, 2017, 539, 24-33.

[12] D. Guo, C. X. Lin, E. N. Hu, L. Shi, F. Soyekwo, Q. G. Zhang, A. M. Zhu and Q. L. Liu, *J. Membr. Sci.*, 2017, 541, 214-223.

[13] A. N. Mondal, Y. He, L. Wu, M. I. Khan, K. Emmanuel, M. M. Hossain, L. Ge and T. Xu, *J. Mater. Chem. A*, 2017, 5, 1022-1027.

[14] M. M. Hossain, J. Hou, L. Wu, Q. Ge, X. Liang, A. N. Mondal and T. Xu, *J. Membr. Sci.*, 2018, 550, 101-109.

[15] S. Kwon, A. H. N. Rao and T.-H. Kim, *J. Power Sources*, 2017, DOI: 10.1016/j.jpowsour.2017.06.047.

[16] J. Wang, Y. Chen, Q. Wei, S. Yang, H. Fang, H. Wei and Y. Ding, *Polymer*, 2017, 112, 288-296.